



Contents lists available at SciVerse ScienceDirect

## Journal of Geochemical Exploration

journal homepage: [www.elsevier.com/locate/jgeoexp](http://www.elsevier.com/locate/jgeoexp)

# Impact of spatial heterogeneities on oxygen consumption in sediments: Experimental observations and 2D numerical modeling

Claude Mügler<sup>a,\*</sup>, Christophe Rabouille<sup>a</sup>, Bruno Bombled<sup>a</sup>, Philippe Montarnal<sup>b</sup>

<sup>a</sup> Laboratoire des Sciences du Climat et de l'Environnement (LSCe/IPSL), CEA-CNRS-UVSQ, Orme des Merisiers, 91191 Gif-sur-Yvette, France

<sup>b</sup> CEA/DEN Saclay, 91191 Gif-sur-Yvette, France

## ARTICLE INFO

## Article history:

Received 15 November 2010

Accepted 30 July 2011

Available online xxx

## Keywords:

Heterogeneity

Reactive transport modeling

Organic-carbon mineralization

Microelectrode

## ABSTRACT

In situ measurements of the sediment geochemical composition performed with high-resolution techniques often exhibit the heterogeneous character of this shallow water environment. Many processes can be responsible for this small-scale variability. Here, we investigate two of these processes: (i) a local deposition of organic matter related to organic aggregates; (ii) a horizontal diffusion of oxygen due to the presence of biological structures, such as burrows or galleries, which result from the activity of macrofauna. In this paper, laboratory experiments and associated 2D numerical simulations are performed together to confirm and to quantify the impact of such small-scale heterogeneities on the dynamics and spatio-temporal variability of biogeochemical cycles in sediments. Both experiments and calculations confirm that a local deposit of organic matter involves an increase in oxygen demand of the sediment as a result of labile organic matter deposit and of its degradation by microorganisms. On the contrary, the presence of biological structures involves lateral diffusion and deeper penetration of oxygen. Burrows act as preferential pathways for fluids and lead to spatially heterogeneous distributions of chemical species. The combination of the results from oxygen microelectrode profiles measured at high lateral resolution in sediments with those from modeling allows to quantify the characteristic distance on which the presence of aggregate or burrow influences the oxygen spatial distribution in the sediment.

© 2011 Elsevier B.V. All rights reserved.

## 1. Introduction

Continental or marine shallow aquatic environments are largely disturbed by human activities (Kennish, 2001). This is mainly due to the large amount of fertilizers used in intensive agriculture and to waste water that is rich in organic matter. Natural biogeochemical cycles undergo important modifications that deteriorate water quality, modify trophic chains to toxic algae and weaken ecosystems. In these environments, biogeochemical cycles are usually characterized by a close coupling between production in the water column and recycling in the sediments. Therefore, sedimentary processes are very important for the evolution of the biogenic and anthropic compounds in the medium. It is consequently essential to understand and quantify their dynamics and their spatio-temporal variability by a combination of experimental measurements and associated modeling efforts.

Until the end of the Nineties, usually a one-dimensional approach was privileged to study sediments, both in their natural environment (Froelich et al., 1979; Gehlen et al., 1997; Jahnke et al., 1982; Reimers,

1987) and in modeling (Bernier, 1980; Boudreau, 1997; Rabouille and Gaillard, 1991; Soetaert et al., 1996; Van Cappellen and Wang, 1996). Innovating techniques allowing high-resolution measurements (Cai and Reimers, 1995; Lansard et al., 2003; Reimers, 1987; Revsbech et al., 1986; Wenzhöfer and Glud, 2004) made it possible to establish a link between vertical oxygen profiles and mineralization of organic matter. Such in situ measurements based on the use of electrochemical microsensors on automated profilers gave access to geochemical distributions on the centimeter scale and revealed a strong variability of the oxygen microprofiles (Dedieu et al., 2007; Glud et al., 2009; Rabouille et al., 2003). The  $O_2$  penetration depth is a good proxy for the benthic microbial activity at a given site. Its value, as measured in situ with high-resolution one-dimensional  $O_2$  microprofiles ranged from 3 to 15 mm (with an average of 4 mm) in the Gulf of Fos in the Mediterranean Sea (Rabouille et al., 2003), and from 2.6 mm to 17.8 mm in the Sagami Bay in Japan (Glud et al., 2009), respectively. Some microprofiles with high values for the penetration-depth of the  $O_2$  into the sediment probably indicated the presence of benthic fauna structures. Both microelectrodes and microoptodes measure the  $O_2$  concentration at a single point, and depth profiles are obtained by a stepwise up or down movement of the sensor through the medium. Glud et al. (1996) proposed a new tool called planar optodes for measuring fine-scale two-dimensional  $O_2$  distributions and dynamics in benthic communities. This new technique yielded results that were

\* Corresponding author. Tel.: +33 1 69089363; fax: +33 1 69087716.  
E-mail address: [claude.mugler@cea.fr](mailto:claude.mugler@cea.fr) (C. Mügler).

in agreement with microelectrode measurements (Glud et al., 1996, 2005) and also revealed heterogeneous oxygen distributions (Glud et al., 2001; Glud et al., 2005; Wenzhöfer and Glud, 2004).

Many processes can be responsible for this small-scale variability such as (i) local deposition of organic matter related to organic aggregates; (ii) enhanced availability of reduced chemical species generated by anoxic oxidation of organic matter in deeper sediments; (iii) horizontal diffusion of oxygen due to the presence of biological structures, such as burrows or galleries which result from macrofauna activity (Rabouille et al., 2003).

The first two processes involve an increase in oxygen demand of the sediment: A labile organic matter deposit increases the oxygen uptake within the sediment (this is a direct consequence of its degradation by microorganisms) and the oxidation of reduced compounds diffusing from the anoxic zone also involves a  $O_2$  consumption. For example, both microelectrode and planar optode measurements showed that the oxygen penetration depths could be locally reduced. This reflected the presence of local hot spots in the oxygen consumption rate associated with fecal mounds (Glud et al., 1996). In (Glud et al., 2005), the small-scale variability in the  $O_2$  penetration depth occurred on the same spatial scales as for aggregates that settled during the investigation period. Other in situ measurements of benthic  $O_2$  concentration performed in the Sagami Bay (Japan) showed that millimeter- to centimeter-sized hot spots with high consumption rates were separated by parcels of low or insignificant  $O_2$  consumption (Glud et al., 2009).

The third process due to the presence of biological structures involves on the contrary lateral diffusion and deeper  $O_2$  penetration. Tubes or burrows left by infauna are often surprisingly stable and can persist for months to years after being vacated (Aller and Aller, 1986). Wenzhöfer and Glud (2004) have shown very impressive examples of spatial and temporal  $O_2$  distributions within sediments influenced by burrowing fauna and photosynthesis. It appeared that with time, burrow structures transported oxygenated water deeper into the sediment, whereas in the absence of any obvious burrow structure, the  $O_2$  penetration depth within the surrounding sediment was only a few millimeters. Even simple visual inspection of the marine sediment surfaces clearly revealed an extensive small-scale heterogeneity (Glud, 2008): Tracks of moving fauna, fecal mounds and burrows, patches of microalgae that might contribute to the benthic  $O_2$  consumption and represent diagenetic hot spots. Numerous experimental investigations documented the importance of macrofauna (Aller and Aller, 1998; Aller and Yingst, 1985; Wenzhöfer and Glud, 2004) or meiofauna (Aller et al., 1998; Aller and Aller, 1992) for benthic diagenesis and solute exchange. While significant, the meiofauna effects were less important than those caused by macrofauna.

One of the shortcomings of the experimental evidence for sediment heterogeneity was that the data represented the sediments as 1D systems with only vertical concentration gradients. The feeding, burrowing, construction and irrigation activities of animals transformed what would otherwise be laterally symmetrical, one-dimensional bodies into complex, time-dependent, three dimensional structures. Therefore, a variety of more sophisticated models were developed to quantify multi-dimensional transport-reaction processes within the bioturbated zone. Aller (1980) was one of the first authors to use a 2D-cylinder geometry to model bioirrigation in muddy sediments with the assumption that bioirrigation was caused by diffusive exchange between the burrow water and the interstitial pore water. In this model, the only physical transport mechanism was molecular diffusion. With this diffusion model, Aller and Yingst (1985) demonstrated that, in the presence of macrofauna, the effective diffusion coefficients were 2–5 times higher than the molecular diffusion value within the upper 8–12 cm of sediment. The magnitude of apparent temporal variation of the diffusion coefficient depended on burrow abundance, size, and depth of burrowing. The same 2D-cylinder geometry and diffusion assumption was also used by Furukawa (2001) in a more

sophisticated reactive model to simulate the geochemical effects of macrofaunal burrow ventilation in the immediate vicinity of burrow walls and at the water–sediment interface. In contrast, other authors proposed to model bioirrigation under the fundamental assumption that advection is the dominant transport mode of interstitial solutes. Indeed, measurements of the  $O_2$  microdistribution around relict tubes revealed an intense passive flushing of the tube structure when it was exposed to ambient flow (Munksby et al., 2002). The extent to which this mechanism was possible depended on the hydraulic conductivity of the sediment, the flow velocity of the overlying water, the geometry of the tube and its relative position in the sediment. For example, in sandy sediments – which are more permeable than muds – Meysman et al. (2006) assumed that the advective pore water flow generated by flushing of worm burrows was the dominant physical transport mechanism. Using a two-dimensional simulation analysis, Cook et al. (2006) also investigated the effects of advective transport due to sediment flushing on rates and measurements of denitrification.

Most of these approaches (Aller, 1980; Aller and Yingst, 1985; Furukawa, 2001; Meysman et al., 2006) implemented a highly simplified model of the natural sediment, that was idealized as a collection of identical average territories inhabited by a single organism. In the 2D tube irrigation model first proposed by Aller (Aller, 1980; Aller and Yingst, 1985; Furukawa, 2001), the average burrow was a straight cylindrical structure. Results from experimental incubations of sediment plugs of varying thickness indicated that simple alterations in the spacing of individual burrow structures in sediments or in the specific geometry of burrow sections entailed significant localized effects on microbial populations, net diagenetic reactions, and elemental cycling. These were solely due to changes in diffusive transport (Aller and Aller, 1998). In the work of Meysman et al. (2006), the actual geometry of the burrow was neglected. They retained only a feeding pocket as the actual location where burrow water was injected into the sediment.

Some of the model simulations were successfully confronted with data obtained from controlled laboratory incubations (Aller, 1980; Meysman et al., 2006) but only conservative tracers were used in the experiments.

In a more recent work, the  $O_2$  consumption rates were derived from in situ concentration measurements with a 2D steady-state mass balance equation for oxygen in the sediment that included transport by molecular diffusion and bioturbation (Glud et al., 2009). This approach yielded very heterogeneous  $O_2$  consumption rates within the surface sediment, characterized by hot spots or zones of intensified activities that were separated by patches of low or insignificant activity. In this approach, experimental  $O_2$  concentrations and resistivity were directly used as input parameters for the net rate of oxygen production or consumption and for the effective diffusive transport coefficient in the model.

We are not aware of any study in the existing literature that would combine oxygen microelectrode data with a modeling of highly reactive tracers such as oxygen. Only conservative tracers were tested in the work of Aller (1980) and Meysman et al. (2006). Simulations performed with a reactive model in the work of Furukawa (2001) were not confronted to experimental data. There was no explicit modeling of the  $O_2$  reactions in the work of Glud et al. (2009). Therefore, in the present paper, we propose to couple controlled experimental and 2D numerical modeling in order to better understand and quantify the impact of small-scale heterogeneities on the dynamics and spatial and temporal variability of biogeochemical cycles in sediments. The originality of this work is to conciliate the data from high-resolution  $O_2$  microelectrode experimental profiles with those of multi-dimensional transport of reactive tracer where both the exact geometry of fauna structures such as burrows and the biogeochemical reactions are explicitly simulated. To achieve this goal we first force separately and specifically certain key processes via laboratory experiments. In a second stage we perform numerical simulations of these experiments. Laboratory experiments

are performed on a natural sediment which has undergone several modifications such as homogenization, creation of artificial structures and additions of organic compounds. 2D numerical simulations of these experiments are performed using a reactive code.

## 2. Laboratory experiments

Laboratory experiments were realized on sediments collected in the Gulf of Fos (Mediterranean Sea), where previous microelectrode profiles measured in situ had revealed the presence of small-scale spatial heterogeneities (Fig. 1 after Rabouille et al. (2003)). First, the sediment was sieved and homogenized. Then, it was put in a 15-cm diameter and 20-cm deep coreliner which was held by a bucket (Fig. 2a). In the coreliner, the sediment was covered by a stagnant 5-centimeter thick water layer. There is no flow within the overlying water and we do not investigate the effects of sediment flushing as done in the work of Munksby et al. (2002) and Cook et al. (2006). Finally, an artificial burrow was created with a diameter of 4 mm and a depth of 2 cm (Fig. 2). A circulation of aerated seawater was imposed inside the burrow in order to maintain the oxygen concentration in the burrow water. On another spot of the core, an organic-matter aggregate in the form of a fish food pill was deposited onto the sediment surface. Measurements were performed using an oxygen microelectrode mounted on a  $x$ - $z$  microprofiler. Both instruments were manufactured by Unisense. Microelectrodes were 50  $\mu\text{m}$  in diameter and were calibrated using Winkler titration in the water overlying the core and zero current in the anoxic zone. Transect were performed at various distances from the organic-matter center (7.5 mm, 10 mm, 12.5 mm, 15 mm, 30 mm) and from the burrow (1–2 mm, 3–4 mm, 8 mm, 16 mm). This allowed to reconstruct 2D-fields of oxygen concentration around the aggregate and around the burrow. These results were then used as data set to which 2D model outputs were compared (see experimental profiles in Figs. 5 and 7).

## 3. The reactive transport model

### 3.1. Numerical code

Mineralization of organic matter in coastal sediments involves many chemical species in pore water. These species are subjected to biogeochemical reactions and are also transported by diffusion or advection in sediments. These two phenomena (chemistry and

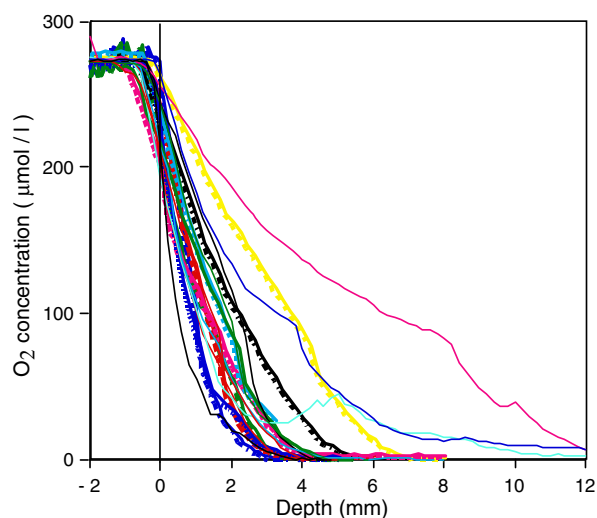


Fig. 1. Oxygen profiles measured in the Gulf of Fos (Mediterranean Sea) showing small-scale spatial heterogeneities (after Rabouille et al. (2003)).

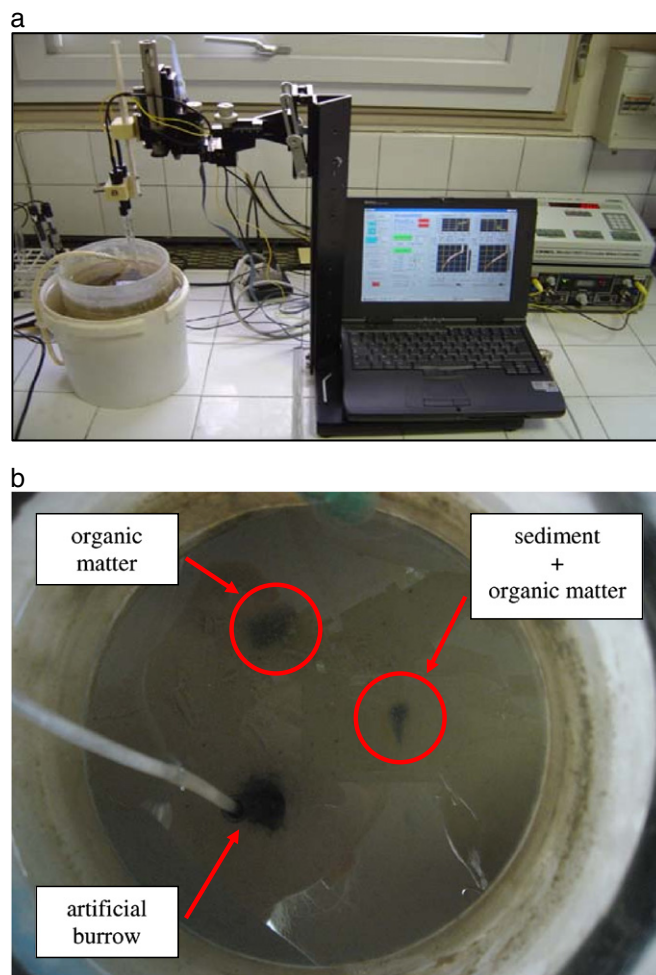


Fig. 2. Experimental set-up (a) global view, (b) zoom on the sediment.

transport) are strongly coupled. To model and simulate such processes in sediments, we used a numerical tool allowing to simulate coupling between geochemistry and transport in porous media (Montarnal et al., 2007). 1D coupled codes have already been used to model the processes that take place in the column of sediments (Giambalvo et al., 2002) but modeling the effects of the presence of 2D heterogeneities in sediments requires to use multidimensional codes (Meile et al., 2003). One of the advantages of the ALLIANCES code we used is precisely its multi-dimensional character (1D, 2D or 3D). The numerical platform ALLIANCES is jointly developed by the French Atomic Commission (CEA), the French Agency for Radioactive Waste Management (ANDRA) and the French Electric Company (EdF) (Montarnal et al., 2006). Its main aim is to allow the simulation of all phenomena governing radioactive waste storage and disposal safety. Therefore, ALLIANCES is not a numerical tool dedicated to simulate phenomena like the early diagenesis but after implementing some additional features it can be used to model reactive transport of various species present in sediments and thus to better understand various processes that take place there.

Modeling reactive transport consists in describing the spatial and temporal evolution of one or several chemical species that are mutually interacting via chemical reactions in liquid or solid phases and are able to be transported. The physical model consists of a set of partial differential equations that describes the transport of species in an aqueous phase that is coupled to a system which gives rise to mutual interactions between the species via chemical reactions. The transport model makes it possible to describe the propagation of elements dissolved in water while subjected to three mechanisms of

migration: Advection, diffusion and kinematic dispersion. For a chemical species  $i$ , the transport equation is given by:

$$\frac{\partial \phi C_i}{\partial t} - \vec{\nabla} \cdot (\vec{D}_i \vec{\nabla} C_i - \vec{U} C_i) = \phi R_i(C_{1\dots n}) + S_i, \quad (1)$$

where  $C_i$  is the total concentration of chemical species  $i$  in aqueous phase,  $\phi$ , the porosity,  $\vec{U}$ , the Darcy velocity,  $\vec{D}_i$ , the diffusion–dispersion tensor,  $R_i(C_{1\dots n})$ , the chemical-reaction term and  $S_i$ , the source term. In the following, we assume that the porosity does not change with time and that the diffusion coefficient  $\vec{D}_i$  is the same for all species. The Darcy velocity is defined as

$$\vec{U} = -\vec{K} \vec{\nabla} h, \quad (2)$$

and is obtained by the resolution of the stationary Darcy equation

$$\vec{\nabla} \cdot \vec{U} = 0, \quad (3)$$

where  $h$  and  $\vec{K}$  are the hydraulic head and the hydraulic-conductivity tensor, respectively.

Transport–Chemistry coupling is solved here by a classical sequential iterative approach (SIA) with iterations between transport and chemistry at each time step. Several methods have been reported that use a simultaneous approach (de Dieuleveult et al., 2009; Hammond et al., 2005; Zhao et al., 2002, 2009) but this requires the development of a global code. The alternative choice adopted in ALLIANCES is to couple existing codes that treat each part: Chemistry (Chess, Phreeqc) and transport (Castem, MT3D). The SIA approach is less memory consuming and it has been proved to be efficient provided the time step is well adapted (Barry et al., 1997; Kanney et al., 2003; Yeh and Tripathi, 1991). Moreover, the SIA method can be improved by acceleration methods (Bouillard et al., 2005).

In the present paper, we use the Cast3M code to solve the transport part (Bernard-Michel et al., 2003) and the Chess code to solve the geochemical part (van der Lee and de Windt, 2002). The chemical-reaction term  $R_i(C_{1\dots n})$  in the transport equation Eq. (1) comes from a geochemical-balance calculation. The geochemical models allow to account for aqueous speciation, dissolution–precipitation when it's in equilibrium or subjected to a kinetic law, and for sorption.

### 3.2. Geochemical modeling

Organic matter is a chemical structure made up of large molecules, with various compounds (proteins, lipids, sugars, amino-acids). Many models were developed in order to simulate the mineralization properties of the organic matter with respect to the oxidants (for example oxygen). As the organic matter is not taken into account in the basic ALLIANCES geochemical database, it was first necessary to define this new species together with the following reactions in which it participates: Degradation of organic matter by aerobic respiration, denitrification, sulfate reduction and metal reduction (see Table 1). In these reactions, the organic matter is noted  $OM_{red}$  but in the ALLIANCES geochemical database, each new reaction must correspond to the definition of a new species. Hence, we used artificial new minerals (noted  $OM_{ppt,i}$  with  $i=1\dots 5$  in Table 1) and artificial aqueous species (noted  $Mn_{ox}$  and  $Fe_{ox}$  in Table 1) to define the various reactions which involve the organic matter. Each of these reactions is a kinetically controlled reaction modeled by using multiplicative Monod kinetics (Giambalvo et al., 2002) as follows:

$$Rate = R \times I \frac{[Ox]}{K_{ox} + [Ox]} [OM_{red}], \quad (4)$$

where  $R$  is the rate constant,  $I$  takes into account the inhibition of a reaction pathway by an energetically more favored pathway,  $[Ox]$  is the total concentration of the electron receptor and  $K_{ox}$  is the half-saturation

**Table 1**

Reactions and associated rate laws added to the basic ALLIANCES geochemical database. The species ( $OM_{ppt,i} + OM_{red}$ ) model the organic matter, of the form  $(CH_2O)_x$ .  $R_{ox}$  and  $R_{anox}$  are the aerobic and anaerobic organic-carbon degradation rates, respectively. Half-saturation constants are taken from Van Cappellen and Wang (1996).

Reaction	Rate law
Aerobic respiration ( $OM_{ppt,1} + OM_{red}$ ) + $2O_2$ $\rightarrow 2CO_3^{2-} + 4H^+$	$R_1 = R_{ox} \times \frac{[O_2]}{K_{O_2} + [O_2]} \times [OM_{red}]$
Denitrification ( $OM_{ppt,2} + OM_{red}$ ) + $1.6NO_3^-$ $\rightarrow 0.4CO_2 + 1.6HCO_3^- +$ $0.8N_2 + 1.2H_2O$	$R_2 = \frac{4}{5} \times R_{anox} \times \frac{[NO_3^-]}{K_{NO_3} + [NO_3^-]} \times \frac{K_{O_2}}{K_{O_2} + [O_2]} \times [OM_{red}]$
Metal reduction ( $OM_{ppt,3} + OM_{red}$ ) + $4Mn_{ox} + 4H^+$ $\rightarrow 2CO_3^{2-} + 4Mn^{2+} + 4H_2O$	$R_3 = 2 \times R_{anox} \times \frac{[Mn_{ox}]}{K_{Mn_{ox}} + [Mn_{ox}]} \times \frac{K_{NO_3}}{K_{NO_3} + [NO_3^-]} \times [OM_{red}]$
( $OM_{ppt,4} + OM_{red}$ ) + $8Fe_{ox} +$ $14CO_2 + 6H_2O$ $\rightarrow 16HCO_3^- + 8Fe^{2+} +$	$R_4 = 4 \times R_{anox} \times \frac{[Fe_{ox}]}{K_{Fe_{ox}} + [Fe_{ox}]} \times \frac{K_{Mn_{ox}}}{K_{Mn_{ox}} + [Mn_{ox}]} \times \frac{K_{NO_3}}{K_{NO_3} + [NO_3^-]} \times \frac{K_{O_2}}{K_{O_2} + [O_2]} \times [OM_{red}]$
Sulfate reduction ( $OM_{ppt,5} + OM_{red}$ ) + $SO_4^{2-}$ $\rightarrow 2HCO_3^- + H_2S$	$R_5 = \frac{1}{2} \times R_{anox} \times \frac{[SO_4^{2-}]}{K_{SO_4} + [SO_4^{2-}]} \times \frac{K_{Fe_{ox}}}{K_{Fe_{ox}} + [Fe_{ox}]} \times \frac{K_{Mn_{ox}}}{K_{Mn_{ox}} + [Mn_{ox}]} \times \frac{K_{NO_3}}{K_{NO_3} + [NO_3^-]} \times \frac{K_{O_2}}{K_{O_2} + [O_2]} [OM_{red}]$
$Mn^{2+}$ and $Fe^{2+}$ oxidation $Fe^{2+} + 0.25O_2 + 1.5H_2O$ $\rightarrow (FeOOH + Fe_{ox}) + 2H^+$ $Mn^{2+} + 0.5O_2 + H_2O$ $\rightarrow (MnO_2 + Mn_{ox}) + 2H^+$	Rate constants ( $s^{-1}$ ) $R_{ox} = 8.625 \times 10^{-6}$ , $R_{anox} = 3.125 \times 10^{-7}$
	Half-saturation constants ( $mol.l^{-1}$ ) $K_{O_2} = 2 \times 10^{-5}$ , $K_{NO_3} = 5 \times 10^{-6}$ , $K_{Mn_{ox}} = 1.6 \times 10^{-2}$ , $K_{Fe_{ox}} = 10^{-1}$ , $K_{SO_4} = 1.6 \times 10^{-3}$

constant. Furthermore, the formulation of the rate of organic-matter degradation contains an explicit dependence on the organic-carbon concentration  $[OM_{red}]$ . The values of the half-saturation constants are taken from Van Cappellen and Wang (1996) (see Table 1). The aerobic and anaerobic organic-carbon degradation rates are supposed to be constant in space because the sediment has been homogenized before the experiments. Other reactions which do not directly involve the organic matter (such as nitrification, sulfide oxidation, mineral formations, ...) are automatically taken into account by the use of the basic ALLIANCES geochemical database.

### 3.3. Numerical simulations

The multidimensional code ALLIANCES has been used to model and simulate laboratory experiments. In the experiments presented in Section 2, the sediment is put into a small coreliner covered by a thin water layer at rest. In our experiments performed in the laboratory at ambient temperature and pressure, we assume that the pore water is incompressible, isothermal and of uniform salinity and that the porosity and permeability remain constant over the sediment domain. Hence, contrary to what happens with the flow in deeper sediments, in this small-scale experiment, we can neglect advective flow caused by the pore fluid pressure gradient (Zhao et al., 2008a) or by sediment flushing (Cook et al., 2006; Munksby et al., 2002). We can also neglect convective flow caused either by the temperature gradient (Nield and Bejan, 1992; Zhao et al., 1997, 2004), by the salinity gradient or by a combination of both (Zhao et al., 2006, 2007). Hence, in the configuration studied here, there is no flow, neither in the water layer, nor in the sediment. The transport of the species is only diffusive. Furthermore, in this experiment without flow, the reactive mass transport system cannot become unstable like a chemical-dissolution front during its propagation within fluid-saturated porous media as reported by Zhao et al. (2008b, 2010a,b).

Two types of simulations have been performed. In a first stage, 2D numerical simulations have been carried out to model the influence of organic-matter aggregates. The sediment is modeled as a 2D-vertical

rectangle under a 1 mm thick seawater layer. For symmetry reasons, it suffices to simulate only half of the domain. The 1200-element mesh is refined near the seawater–sediment interface and near the left hand side where the organic-matter aggregate is located (in red in Fig. 3a): The vertical grid spacing increases from 0.4 mm at the sediment surface to 16 mm at the lower boundary of the model domain. The horizontal grid spacing increases from 0.5 mm to 4 mm (Fig. 3a). The initial chemical compositions of the seawater and of the sediment are different, with initially no oxygen in the sediment pore water (see Table 2). The presence of OM aggregate is modeled by imposing a larger concentration of the  $OM_{red}$  species at the top boundary: The value of  $[OM_{red}]$  is equal to  $4 \times 10^{-3} \text{ mol.l}^{-1}$  within and to  $8 \times 10^{-4} \text{ mol.l}^{-1}$  outside the aggregate, respectively.

In a second stage, 2D numerical simulations are performed to model the influence of geometric heterogeneities such as burrow. The system simulated is presented in Fig. 3b. Only half of the domain is simulated. The sea–sediment interface is exactly located at the position determined in the laboratory: It takes into account the 10 mm wide depression in the sediment due to the burrow. The burrow itself is only a few millimeters deep (in red in Fig. 3b). A seawater layer of 1 mm thickness on top of the sediment is incorporated into the model. The  $80 \times 80 \text{ mm}^2$  porous medium simulated is a 1316-element mesh bi-dimensional system (see Fig. 3b). The mesh is refined near the seawater–sediment and burrow–sediment interfaces: The vertical grid spacing increases from 0.4 mm at the sediment surface to 3.5 cm at the lower boundary of the model domain. The initial chemical compositions of the seawater and the sediment are different, with no oxygen in the sediment pore water (see Table 2). Oxygen-rich seawater is imposed at the top of the sediment. The same Dirichlet-type boundary condition is imposed at the left-lateral boundary to model the burrow.

#### 4. Results and discussion

Fig. 4 displays a  $50 \times 15 \text{ mm}^2$  zoom of the simulated 2D vertical map of  $O_2$  concentration when an organic-matter aggregate is present. The maps are stationary, i.e. steady-state conditions have been reached.

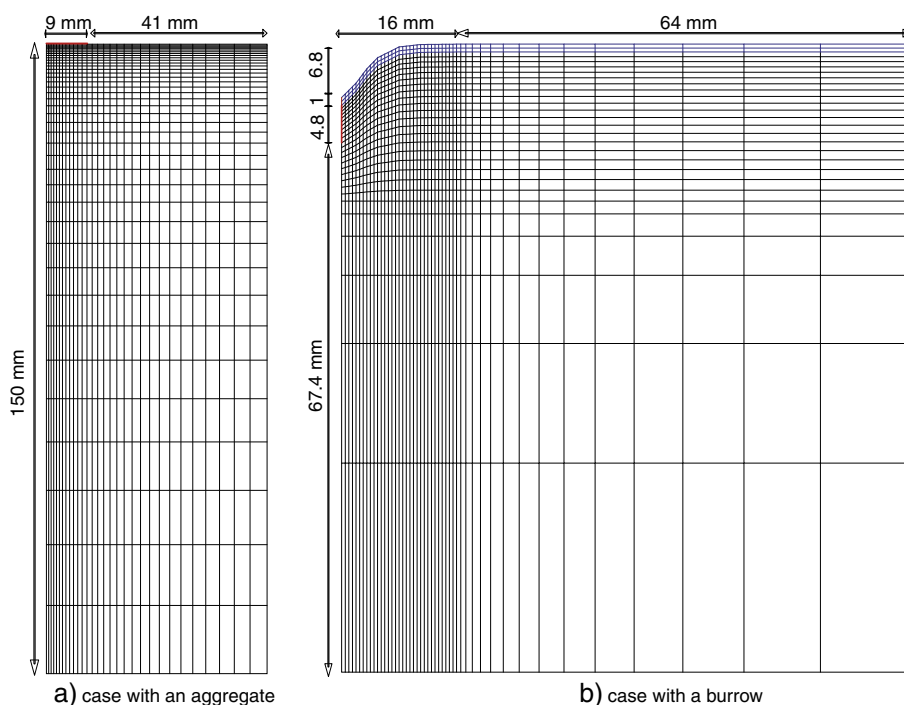


**Fig. 3.** Simulated porous media geometries and associated meshes: (a) Case of an organic-matter aggregate. (b) Case of a burrow. Blue and black zones correspond to the 1 mm deep seawater zone and the 80 mm deep sediment, respectively. The red segment corresponds to the burrow–sediment interface where Dirichlet-boundary conditions are imposed. (For interpretation of the references to color in this figure legend, the reader is referred to the web version of this article.)

**Table 2**

Initial and boundary conditions for the simulation. Concentrations are expressed in  $\text{mol.l}^{-1}$  and ‘–’ stands for concentrations which are not fixed.

	Injected seawater	Seawater zone	Sediment zone
<i>Geochemical data</i>			
<i>pH</i>	7.9	7.38	7.38
$[O_2(aq)]$	$2.28 \times 10^{-4}$	–	–
$[CO_2(aq)]$	$1.82 \times 10^{-3}$	$1.82 \times 10^{-3}$	–
$[NO_3^-]$	$1.0 \times 10^{-6}$	$1.0 \times 10^{-6}$	–
$[SO_4^{2-}]$	$2.8 \times 10^{-2}$	$2.8 \times 10^{-2}$	$1.0 \times 10^{-2}$
$[NH_4^+]$	$1.0 \times 10^{-6}$	$1.0 \times 10^{-6}$	$7.5 \times 10^{-4}$
$[Ca^{2+}]$	$1.009 \times 10^{-2}$	$1.009 \times 10^{-2}$	–
$[Mn^{2+}]$	0.	0.	–
$[Fe^{2+}]$	0.	0.	–
$[OM_{red}]$	$8.0 \times 10^{-4}$	$8.0 \times 10^{-4}$	$8.0 \times 10^{-4}$
$[FeOOH]$	–	–	$2.5 \times 10^{-3}$
$[MnO_2]$	–	–	$4. \times 10^{-5}$
$[Fe_{ox}]$	–	–	$2.5 \times 10^{-3}$
$[Mn_{ox}]$	–	–	$4. \times 10^{-5}$
$[OM_{ppt,i}]$	0.	0.	1.
$[Calcite]$	–	–	$5.0 \times 10^{-2}$
<i>Other parameters</i>			
$\phi$	1.0	1.0	0.9
$D$	$10^{-9}$	$10^{-9}$	$3.0 \times 10^{-10}$
$U$	0.	0.	0.

The sediment is completely anoxic except within a thin zone at the sediment–water interface which becomes thinner and thinner near the aggregate. Fig. 5 confirms this behavior. It provides vertical profiles of the oxygen concentration obtained from experiments (symbols) and 2D simulations (lines) at various distances from the aggregate center. The experimental and numerical results are in a quite good agreement. They clearly show the influence of organic-matter aggregates on the oxygen profiles: In the absence of aggregate, the oxygen diffuses about 5 mm downwards, while in the presence of aggregate, the oxygen penetrates less than 1 mm and the oxygen gradient is larger. Laterally, the aggregate influences the  $O_2$  distribution within a radius of a few centimeters, i.e. on a distance equal to 1 or 2 times the aggregate

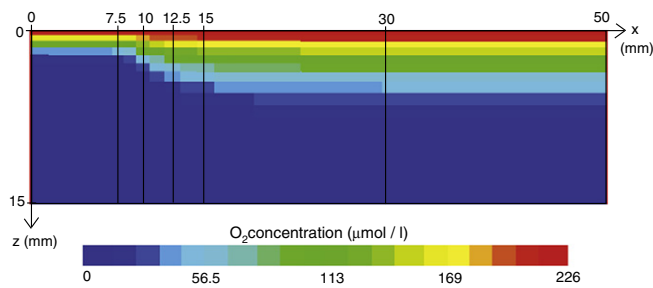


**Fig. 4.** Case of an organic-matter aggregate. Zoom of the simulated oxygen 2D map: only a  $50 \times 15 \text{ mm}^2$  zone close to the aggregate is shown here. Vertical black lines show the location of the vertical profiles given in Fig. 5.

dimension. This enhanced consumption of oxygen is linked to a larger mineralization within the organic aggregate which increases oxygen demand and stops oxygen penetration. The slight discrepancy between the model calculations and the experimental data for the profiles through the aggregate can be attributed to numerical diffusion due to grid spacing.

Fig. 6 displays a  $16 \times 16 \text{ mm}^2$  zoom of the simulated 2D vertical map of the  $\text{O}_2$  concentration in the presence of a burrow structure. The sediment is completely anoxic except on a few millimeters thick zone around the burrow and at the sediment–water interface. Except for a region very close to the burrow (see the red tail), the oxygen penetration looks very homogeneous over the whole 2D plot, suggesting a limited spatial influence of the burrow on oxygen penetration and flux. Fig. 7 confirms this suggestion. It provides vertical profiles of the oxygen concentration obtained from experiments (symbols) and 2D simulations (lines) at various distances from the burrow. At 16 mm from the burrow,  $\text{O}_2$  profiles (red curve and red circles in Fig. 7) are the same as those obtained at 30 mm from the aggregate center (red curve and red circles in Fig. 5). Close to the burrow, the measured oxygen profile follows a “S-shaped” curve and oxygen penetrates deeper by 4 mm in sediment. The penetration length is very sensitive to the burrow depth because it depends on oxygen lateral diffusion. Simulation at a distance of 1 and 2 mm from the burrow shows a similar trend with a “S-shape” profile and deeper penetration.

Experimental and simulated profiles given in Figs. 5 and 7 clearly show that the presence of organic-matter aggregate or burrow modifies the oxygen dynamics: It confers a two-dimensional character to the oxygen distribution in the sediment.

These results can be compared to the in situ studies of Rabouille et al. (2003) performed in the Gulf of Fos in 2000–2001. The authors showed that the sediment was a mosaic of hot spots where the oxygen consumption is higher. The profiles are steep and they penetrate deeper

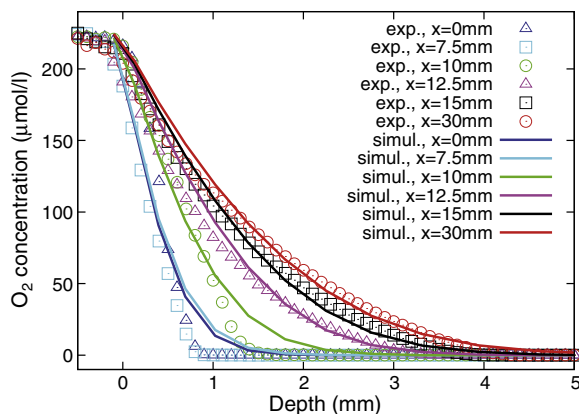


**Fig. 5.** Case of an organic-matter aggregate. Oxygen profiles at various distances from the aggregate, obtained from measurements (symbols) and from modeling (lines).

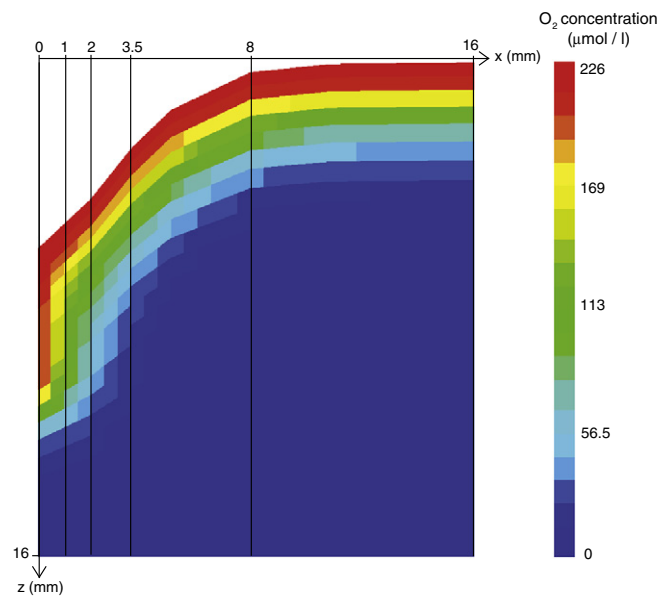


**Fig. 6.** Case of a burrow. Zoom of the simulated oxygen 2D map: only a  $16 \times 16 \text{ mm}^2$  zone close to the burrow is shown here. Vertical black lines show the location of the vertical profiles given in Fig. 7.

into the sediment. According to the 2D model for the processes presented in this study, we can attribute steeper oxygen profiles to organic hot spots and deeper penetrating profiles to lateral diffusion of oxygen from burrows. Whereas the penetration depth is 4 mm on average, a few profiles exhibited a penetration depth that ranged between 8 and 10 mm (Rabouille et al., 2003). This could be attributed to a rapid smoothing out of the deeper penetration (over a lateral distance of 2–3 mm) and to the limited number of burrows at the sediment surface. The investigation of the local variation in the vertical distributions of the solutes within the bioturbated zone of hemipelagic sediments from the Panama Basin also showed that the concentrations of the solutes could vary laterally by a factor of 2–3 within the same depth interval (Aller et al., 1998). X-radiographs of sediment core confirmed that the sediment was a meshwork of biogenic structures: Small burrows of millimetric diameter alternated with larger 1–2 cm diameter burrows. Other simulations (not shown here) illustrated the influence of the burrow geometry (width, depth) on the oxygen spatial distribution. In the simulations presented in Figs. 6 and 7, we took the exact geometry of the artificial burrow. The significant impact that small changes of burrow geometry can have on the reaction balance, has already been noted by Aller and Aller (1998). Their

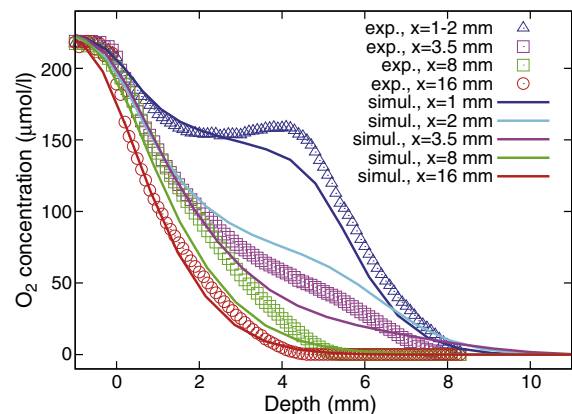


**Fig. 7.** Case of a burrow. Oxygen profiles at various distances from the burrow, obtained from measurements (symbols) and from modeling (lines).

experiments designed to simulate different degrees of diffusive exchange (and thereby infaunal abundances or activity) demonstrated a regular and strong dependence of anaerobic remineralization on diffusive transport. For example, the net production of  $NH_4^+$ ,  $HPO_4^{2-}$ ,  $I^-$  and  $Mn_2^+$  increased when the effective distance between burrows became <2 cm within an otherwise identical anoxic sediment. In our case, the presence of a burrow modifies the  $O_2$  distribution on a lateral scale comprised between 8 and 16 mm, i.e. about 1 or 2 times the width of the geometric perturbation of the sediment due to the burrow. In another setting (Sagami Bay, 1450 m deep), Glud et al. (2005, 2009) concluded that the heterogeneity of the oxygen demand and oxygen penetration into the sediment was linked to “an inhomogeneous distribution of electron donors” (e.g. organic matter). Their combined data set reflected extensive small-scale variability in the  $O_2$  penetration depth with values ranging from 2.6 mm to 17.8 mm: Within a distance of a few centimeters the  $O_2$  penetration could vary by a factor of 6 (Glud et al., 2009). A detailed autocorrelation analysis on the combined data set revealed that the small-scale variability in  $O_2$  penetration depth varied with patch sizes of about 2 cm in diameter. This is of the same spatial scales as for aggregates that settled during the investigation period (Glud et al., 2005). Calibrated experiments and simulations presented in the present paper confirm the influence of aggregates on spatial scales of the same order as their size. Results suggest that hot spots of organic matter can be part of the causes of heterogeneity, but that deep penetrating profiles can be linked to macrofaunal burrows and lateral diffusion of oxygen instead of lower organic-matter mineralization.

## 5. Conclusion

In the present paper, we have presented a combination of high-resolution oxygen microelectrode profiles measured in sediments with modeling. Laboratory experiments and associated numerical simulations confirmed the important role of biogenic structures and organic-matter aggregates on the dynamics and spatial variability of biogeochemical cycles. Burrows act as preferential pathways for fluids and lead to spatially heterogeneous distributions of the chemical species. In addition, it illustrates the use of a multidimensional reactive code that couples geochemistry and transport in porous media and explicitly takes into account spatial heterogeneities in order to model and explain processes of recycling of organic matter in the first layers of sediments. Future work will consist in using this 2D-reactive code to model in situ measurements such as  $O_2$  2D-maps obtained from planar optodes.

## Acknowledgments

This work was supported by the EC2CO-program from the Institut National des Sciences de l'Univers (INSU-France). We would like to thank two anonymous reviewers for their helpful comments and constructive criticism.

## References

Aller, R.C., 1980. Quantifying solute distributions in the bioturbated zone of marine sediments by defining an average microenvironment. *Geochimica et Cosmochimica Acta* 44, 1955–1965.

Aller, J.Y., Aller, R.C., 1986. Evidence for localized enhancement of biological associated with tube and burrow structures in deep-sea sediments at the HEEBLE site, western North Atlantic. *Deep-Sea Research I* 33, 755–790.

Aller, R.C., Aller, J.Y., 1992. Meiofauna and solute transport in marine muds. *Limnology and Oceanography* 37, 1018–1033.

Aller, R.C., Aller, J.Y., 1998. The effect of biogenic irrigation intensity and solute exchange on diagenetic reaction rates in marine sediments. *Journal of Marine Research* 56, 905–936.

Aller, R.C., Yingst, J.Y., 1985. Effects of the marine deposit-feeders *Heteromastus filiformis* (Polychaeta), *Macoma balthica* (Bivalvia), and *Tellina texana* (Bivalvia) on averaged sedimentary solute transport, reaction rates, and microbial distributions. *Journal of Marine Research* 43, 615–645.

Aller, R.C., Hall, P.O.J., Rude, P.D., Aller, J.Y., 1998. Biogeochemical heterogeneity and suboxic diagenesis in hemipelagic sediments of the Panama Basin. *Deep-Sea Research I* 45, 133–165.

Barry, D.A., Miller, C.T., Culligan, P.J., Bajracharya, K., 1997. Analysis of split operator methods for nonlinear and multispecies groundwater chemical transport models. *Mathematics and Computers in Simulation* 43, 331–341.

Bernard-Michel, G., Le Potier, C., Becchantini, A., Chrebi, M., 2003. The ANDRA Couplex 1 test-case: comparisons between finite element, mixed-hybrid-finite element and finite volume discretizations with CAST3M. *Computational Geosciences* 8, 187–201.

Berner, R.A., 1980. *Early Diagenesis: A Theoretical Approach*. Princeton University Press, Princeton.

Boudreau, B.P., 1997. *Diagenetic models and their implementation*. Springer, Berlin.

Bouillard, N., Montarnal, P., Herbin, R., 2005. Development of numerical methods for the reactive transport of chemical species in a porous media: a nonlinear conjugate gradient method. *Proceedings of the International Conference on Computational Methods for Coupled Problems in Science and Engineering*, Santorini, Greece May 2005.

Cai, W.J., Reimers, C.E., 1995. Benthic oxygen flux, bottom water oxygen concentration and core top organic carbon content in the deep northeast Pacific Ocean. *Deep-Sea Research I: Oceanographic Research Papers* 36, 121–128.

Cook, P.L.M., Wenzhöfer, F., Rysgaard, S., Galaktionov, O.S., Meysman, F.J.R., Eyre, B.D., Cornwell, J., Huettel, M., Glud, R.N., 2006. Quantification of denitrification in permeable sediments: insights from a two-dimensional simulation analysis and experimental data. *Limnology and Oceanography: Methods* 4, 294–307.

de Dieuleveult, C., Erhel, J., Kern, M.A., 2009. Global strategy for solving reactive transport equations. *Journal of Computational Physics* 228, 6395–6410.

Dedieu, K., Rabouille, C., Thouzeau, G., Jean, F., Chauvaud, L., Clavier, J., Mesnage, V., Ogier, S., 2007. Benthic  $O_2$  distribution and dynamics in a Mediterranean lagoon (Thau, France): an in situ microelectrode study. *Estuarine, Coastal and Shelf Science* 72, 393–405.

Froelich, P.N., Klinkhammer, G.P., Bender, M.L., Luedtke, N.A., Heath, G.R., Cullen, D., Dauphin, P., Hammond, D., Hartman, B., Maynard, V., 1979. Early oxidation of organic matter in pelagic sediments of the eastern equatorial Atlantic: suboxic diagenesis. *Geochimica et Cosmochimica Acta* 43, 1075–1090.

Furukawa, Y., 2001. Biogeochemical consequences of macrofauna burrow ventilation. *Geochemical Transactions* 11. doi:10.1039/b108381c.

Gehlen, M., Rabouille, C., Guidi-Guilvard, L.D., Ezat, U., 1997. Drastic changes in deep-sea sediment porewater composition induced by episodic input of organic matter. *Limnology and Oceanography* 42, 980–986.

Giambalvo, E.R., Steefel, C.I., Fischer, A.T., Rosenbberg, N.D., Wheat, C.G., 2002. Effect of fluid-sediment reaction on hydrothermal fluxes of major elements, eastern flank of the Juan de Fuca Ridge. *Geochimica et Cosmochimica Acta* 66, 1739–1757.

Glud, R.N., 2008. Oxygen dynamics of marine sediments. *Marine Biology Research* 4, 243–289.

Glud, R.N., Ramsing, N.B., Gundersen, J.K., Klimant, I., 1996. Planar optodes: a new tool for fine scale measurements of two-dimensional  $O_2$  distribution in benthic communities. *Marine Ecology Progress Series* 140, 217–226.

Glud, R.N., Tengberg, A., Kuhl, M., Hall, P., Klimant, I., Holst, G., 2001. An in situ instrument for planar optode measurements at benthic interfaces. *Limnology and Oceanography* 46, 2073–2080.

Glud, R.N., Wenzhöfer, F., Tengberg, A., Middelboe, M., Oguri, K., Kitazato, H., 2005. Distribution of oxygen in surface sediments from central Sagami Bay, Japan: in situ measurements by microelectrodes and planar optodes. *Deep-Sea Research I* 52, 1974–1987.

Glud, R.N., Stahl, H., Berg, P., Wenzhöfer, F., Kitazato, H., 2009. In situ microscale variation in distribution and consumption of  $O_2$ : a case study from a deep ocean margin sediment (Sagami Bay, Japan). *Limnology and Oceanography* 54, 1–12.

Hammond, G., Valocchi, A., Lichtner, P., 2005. Application of Jacobian-free Newton-Krylov with physics-based preconditioning to biogeochemical transport. *Advances in Water Resources* 28, 359–376.

Jahnke, R., Heggie, D., Emerson, S., Grundmanis, V., 1982. Pore waters of the central Pacific Ocean: nutrient results. *Earth and Planetary Science Letters* 61, 233–256.

Kanney, J.F., Miller, C.T., Kelley, C.T., 2003. Convergence of iterative split operator approaches for approximating nonlinear reactive transport problems. *Advances in Water Resources* 26, 247–261.

Kennish, M.J., 2001. *Practical handbook of marine science*, 3rd ed. CRC Press, Boca Raton, Florida.

Lansard, B., Rabouille, C., Massias, D., 2003. Variability in benthic oxygen fluxes during the winter-spring transition in coastal sediments: an estimation by in situ microelectrodes and laboratory minielectrodes. *Oceanologica Acta* 26, 269–279.

Meile, C., Tuncay, K., Van Capellen, P., 2003. Explicit representation of spatial heterogeneity in reactive transport models: application to biorrigated sediments. *Journal of Geochemical Exploration* 78–79, 231–234.

Meysman, F.J.R., Galakyonov, O.S., Gribsholt, B., Middelburg, J.J., 2006. Bioirrigation in permeable sediments: advective pore-water transport induced by burrow ventilation. *Limnology and Oceanography* 51, 142–156.

Montarnal, P., Bengaouer, A., Chavant, C., Loth, L., 2006. ALLIANCES: simulation platform for nuclear waste disposal. *Proceedings of the XVI International Conference on Computational Methods in Water Resources*, Copenhagen, Denmark, June 2006.

Montarnal, P., Mügler, C., Colin, J., Descostes, M., Dimier, A., Jacquot, E., 2007. Presentation and use of a reactive transport code in porous media. *Physics and Chemistry of the Earth* 32, 507–517.

Munksby, N., Benthien, M., Glud, R.N., 2002. Flow-induced flushing of relict tube structures in the central Skagerrak (Norway). *Marine Biology* 141, 939–945.

Nield, D.A., Bejan, A., 1992. *Convection in Porous Media*. Springer-Verlag, New York.

- Rabouille, C., Gaillard, J.-F., 1991. Towards the EDGE: Early Diagenetic Global Explanation. A model depicting the early diagenesis of organic matter, O<sub>2</sub>, NO<sub>3</sub>, Mn, and PO<sub>4</sub>. *Geochimica et Cosmochimica Acta* 55, 2511–2525.
- Rabouille, C., Denis, L., Dedieu, K., Stora, G., Lansard, B., Grenz, C., 2003. Oxygen demand in coastal marine sediments: comparing in situ microelectrodes and laboratory core incubations. *Journal of Experimental Marine Biology and Ecology* 285/286, 49–69.
- Reimers, C.E., 1987. An in situ microprofiling instrument for measuring interfacial porewater gradients: methods and oxygen profiles from the North Pacific Ocean. *Deep-Sea Research A: Oceanographic Research Papers* 34, 2019–2035.
- Revsbech, N.P., Madsen, B., Jørgensen, B.B., 1986. Oxygen production and consumption in sediments determined at high spatial resolution by computer simulation of oxygen microelectrode data. *Limnology and Oceanography* 31, 293–304.
- Soetaert, K., Herman, P.M.J., Middelburg, J.J., 1996. A model of early diagenetic processes from the shelf to abyssal depths. *Geochimica et Cosmochimica Acta* 60, 1019–1040.
- Van Cappellen, P., Wang, Y., 1996. Cycling of iron and manganese in surface sediments: a general theory for the coupled transport and reaction of carbon, oxygen, nitrogen, sulfur, iron and manganese. *American Journal of Science* 296, 197–243.
- van der Lee, J., de Windt, L., 2002. Chess Tutorial and Cookbook, version 3.0, ENSMP-CIG LHM/RD/02/13.
- Wenzhöfer, F., Glud, R.N., 2004. Small-scale spatial and temporal variability in coastal benthic dynamics: effects of fauna activity. *Limnology and Oceanography* 49, 1471–1481.
- Yeh, G.-T., Tripathi, V.S., 1991. A model for simulating transport of reactive multispecies components: model development and demonstration. *Water Resources Research* 27, 3075–3094.
- Zhao, C., Mühlhaus, H.B., Hobbs, B.E., 1997. Finite element analysis of steady-state natural convection problems in fluid-saturated porous media heated from below. *International Journal for Numerical and Analytical Methods in Geomechanics* 21, 863–881.
- Zhao, C., Lin, G., Hobbs, B.E., Wang, Y., Mühlhaus, H.B., Ord, A., 2002. Finite element modeling of reactive fluids mixing and mineralization in pore-fluid saturated hydrothermal/sedimentary basins. *Engineering Computations* 19, 364–387.
- Zhao, C., Hobbs, B.E., Ord, A., Peng, S., Mühlhaus, H.B., Liu, L., 2004. Theoretical investigation of convective instability in inclined and fluid-saturated three-dimensional fault zones. *Tectonophysics* 387, 47–64.
- Zhao, C., Hobbs, B.E., Ord, A., Kühn, M., Mühlhaus, H.B., Peng, S., 2006. Numerical simulation of double-diffusion driven convective flow and rock alteration in three-dimensional fluid-saturated geological fault zones. *Computer Methods in Applied Mechanics and Engineering* 195, 2816–2840.
- Zhao, C., Hobbs, B.E., Ord, A., Hornby, P., Peng, S., Liu, L., 2007. Mineral precipitation associated with vertical fault zones: the interaction of solute advection, diffusion and chemical kinetics. *Geofluids* 7, 3–18.
- Zhao, C., Hobbs, B.E., Ord, A., 2008a. *Convective and Advective Heat Transfer in Geological Systems*. Springer, Berlin.
- Zhao, C., Hobbs, B.E., Hornby, P., Ord, A., Peng, S., Liu, L., 2008b. Theoretical and numerical analyses of chemical-dissolution front instability in fluid-saturated porous rocks. *International Journal for Numerical and Analytical Methods in Geomechanics* 32, 1107–1130.
- Zhao, C., Hobbs, B.E., Ord, A., 2009. *Fundamentals of Computational Geoscience: Numerical Methods and Algorithms*. Springer, Berlin.
- Zhao, C., Hobbs, B.E., Ord, A., 2010a. Theoretical analyses of nonaqueous phase liquid dissolution-induced instability in two-dimensional fluid-saturated porous media. *International Journal for Numerical and Analytical Methods in Geomechanics* 34, 1767–1796.
- Zhao, C., Hobbs, B.E., Ord, A., 2010b. Theoretical and numerical investigation into roles of geofluid flow in ore forming systems: integrated mass conservation and generic model approach. *Journal of Geochemical Exploration* 106, 251–260.